IOP PUBLISHING NONLINEARITY

Nonlinearity **20** (2007) 1283–1298 doi:10.1088/0951-7715/20/5/012

Resonances for weak coupling of the unfolding of a saddle-node periodic orbit with an oscillator

C Baesens and R S MacKay

Mathematics Institute, University of Warwick, Coventry CV4 7AL, UK

Received 1 December 2006, in final form 25 March 2007
Published 17 April 2007
Online at stacks.iop.org/Non/20/1283

Recommended by D Treschev

Abstract

For a family of continuous-time dynamical systems with two angle variables, a *resonance* is a set of parameter values such that some integer combination of the (lifted) angles remains bounded for some orbits. For weak coupling of an unfolding of a saddle-node periodic orbit with an oscillator, it is shown that the low order resonances have at least a certain amount of bifurcation structure. Furthermore, define a *Chenciner bubble* to be the complement of the set of parameters near a resonance for which there is an attractor–repellor pair consisting of two C^1 invariant tori, or a C^1 invariant torus attracting from one side and repelling from the other, or locally empty non-wandering set. The low order Chenciner bubbles are shown to have at least a certain structure. Chenciner's results for resonances in the unfolding of a degenerate Neimark–Sacker bifurcation can be seen as a special case of ours.

Mathematics Subject Classification: 34C15, 34C23

1. Introduction

Chenciner's seminal work on the unfolding of a map with a degenerate Neimark–Sacker fixed point [Ch, Yo] ends by studying the resonances that occur. To define a resonance in that context, take an angle variable $\theta \in \mathbb{T} = \mathbb{R}/\mathbb{Z}$ around the fixed point and discrete time $n \in \mathbb{Z}$. For $(p, q) \in \mathbb{Z} \times \mathbb{N}$ the (p, q)-*resonance* is the set of parameter values for which there is an orbit with $q\theta_n - np$ bounded, for a lift of the map to the universal cover of the punctured plane. Chenciner obtained a flow approximation for families of maps near a resonance, and with Gasull and Llibre [CGL] obtained its bifurcation diagram and the shape of the associated *Chenciner bubble*, the complement of the set of parameters for which the flow approximation has an attractor–repellor pair (for the general concept, see e.g. [Co]) consisting of two C^1 invariant circles, or a C^1 invariant circle attracting from one side and repelling from the other, or locally empty non-wandering set. By suspension, the same conclusions hold for the unfolding of a flow with a degenerate Neimark–Sacker periodic orbit.

Extensions of Chenciner's work have been made in some directions, e.g. [TW] and references in [BNRSW].

Here we generalize from Chenciner's local context to the global context of interaction between a saddle-node of periodic orbits for a vector field and a limit-cycle oscillator which is *not* assumed to be close to a Hopf bifurcation. To make progress we assume weak coupling, thus a different form of locality, yet we obtain a significant extension of Chenciner's results.

The results are that the simplest robust bifurcation diagram for a 'flow approximation' to the Poincaré map of a two-parameter family of such systems is figure 5, the simplest robust form for its Chenciner bubble is figure 9 and various bifurcation curves are fattened slightly for the true family as shown in figure 11.

This paper is an outgrowth of our work on three coupled oscillators [BGKM]. Our motivation was to understand those parts of the boundary of partial mode-locking strips corresponding to saddle-node of periodic orbits for a flow approximation for three coupled oscillators, without the unnecessary complication of the third angle direction. Comments on this situation are made in the conclusion.

2. Starting point

We start from a family of vector fields unfolding an elementary saddle-node of periodic orbits, and an uncoupled oscillator. *Elementary* means that the quadratic term in the normal form for the return map to a transverse section is non-zero and that the return time has non-zero derivative along the section. It can be unfolded with two parameters: one to unfold the saddle-node for the return map and the other to vary the return time. Normally the second would not be considered relevant for the qualitative dynamics, but our aim is to couple with an oscillator and study resonance with it, so the ratio of return time to period of the oscillator plays an essential role.

Concretely, let I be an interval containing 0 and choose as an uncoupled case a C^r family of vector fields on $\mathbb{T} \times I \times \mathbb{T}$, with r large (three suffices, but the higher it is the better we can reduce dependence on one combination of angles) of the form

$$\begin{aligned} \dot{x} &= \beta + y/\gamma + HOT(y) \\ \dot{y} &= \alpha - y^2 + HOT(y) \\ \dot{z} &= 1, \end{aligned} \tag{1}$$

where $HOT(y)$ denotes higher order terms in y which may depend on α, β, γ and have period 1 in x. Note that the parameter γ can be taken positive (else reflect the signs of x and β) but its absolute value cannot be changed by scaling, so we are forced to consider at least a three-parameter family from the start; nevertheless we will treat γ as constant. The higher order terms cannot in general be chosen independent of x because that would imply the return map to a transverse section for $\alpha > 0$ has trivial Mather invariant (the Mather invariant of an orientation-preserving diffeomorphism of an interval between neighbouring non-degenerate fixed points is an infinite-dimensional invariant of smooth conjugacy, e.g. [AY, IY]). The dependence on x, however, can be pushed to arbitrarily high order in α in the range of interest ($|y|$ of order $\sqrt{\alpha}$, β not small) by a sequence of averaging transformations (cf [SV, GH, LM]).

Then consider the effect of adding a general small smooth perturbation to each component of (1), depending on all the three components (x, y, z). We denote the size of the perturbation by ε and consider it small and fixed. Since this can produce arbitrarily complicated bifurcation diagrams, our strategy is to consider the simplest (and sometimes second simplest) codimension-2 robust cases at each stage of the analysis. The conclusion is that all bifurcation

diagrams contain at least all the features we obtain (where features of higher codimension are considered to contain all the features of their unfoldings).

In principle it would be good to formalize the notion of 'simplest' bifurcation diagram by defining a partial order on them and proving results about the minimal elements of this partial order (cf the theory of pseudo-Anosov maps [AF,Ha]), but as in [BGKM,BGKM2] our treatment will be informal.

3. Reduction from (p, q)-resonance to $(0, 1)$

In the context of the vector field (1) and its perturbations, for $(p, q) \in \mathbb{Z} \times \mathbb{N}$, (p, q)-resonance means existence of an orbit for which $qx - pz$ is bounded in the universal cover $\mathbb{R} \times I \times \mathbb{R}$. For ε small enough (depending on (p, q)), we can change angle variables to reduce to the case $(0, 1)$. The strategy is based on Fried's idea of 'flow equivalence' [Fr] (cf appendix A of [BGKM]).

Without loss of generality, take (p, q) to be relatively prime. Let p'/q' be the penultimate convergent in the continued fraction expansion of p/q, and $\sigma = q'p - p'q \in \{\pm 1\}$. Then

$$X = qx - pz$$
$$Y = qy$$
$$Z = \sigma(q'x - p'z)$$

are new coordinates on $\mathbb{T} \times I \times \mathbb{T}$ (with an interval I of q times the length). For the uncoupled system (1) we obtain

$$\dot{X} = q\left(\beta + \frac{Y}{q\gamma} + HOT(Y)\right) - p$$
$$\dot{Y} = q\left(\alpha - \frac{Y^2}{q^2} + HOT(Y)\right)$$
$$\dot{Z} = \frac{1}{q} + \sigma q'\left(\beta - \frac{p}{q} + \frac{Y}{q\gamma} + HOT(Y)\right),$$

where the high order terms depend on X, Z through only the combination $x = pZ - \sigma p' X$. In particular, if $\beta - p/q$ is small enough and $|Y| < \frac{\gamma}{2q'}$ then $\dot{Z} \geqslant \frac{1}{2q} > 0$, so we can use $\tau = Z$ as a new time variable. Then the equations of motion become

$$\frac{\mathrm{d}X}{\mathrm{d}\tau} = \tilde{\beta} + \frac{Y}{\tilde{\gamma}} + O(Y^2, \tilde{\beta}Y, \tilde{\beta}^2)$$
$$\frac{\mathrm{d}Y}{\mathrm{d}\tau} = \tilde{\alpha} - Y^2 + O(Y^3, \tilde{\beta}Y^2, \tilde{\alpha}Y, \tilde{\alpha}\tilde{\beta})$$
$$\frac{\mathrm{d}Z}{\mathrm{d}\tau} = 1$$

with

$$\tilde{\beta} = q^2\left(\beta - \frac{p}{q}\right)$$
$$\tilde{\alpha} = q^2\alpha$$
$$\tilde{\gamma} = \gamma/q,$$

where the remainder terms may depend weakly on x but only at high order in $\tilde{\alpha}$. Near-identity parameter and coordinate changes can be made to remove the $\tilde{\beta}Y$, $\tilde{\beta}^2$, $\tilde{\beta}Y^2$, $\tilde{\alpha}Y$, $\tilde{\alpha}\tilde{\beta}$ terms.

Thus we have reduced the uncoupled system near a (p, q)-resonance to that for $(0, 1)$ with rescaled parameters $\tilde{\alpha}, \tilde{\beta}, \tilde{\gamma}$, the only change being that the high-order in α period-1 dependence of the higher order terms in Y is on $pZ - \sigma p' X$ rather than X. Weak coupling ε produces a perturbation of this by terms dependent on (X, Y, Z).

4. Flow approximation

Using the result of the previous section we now restrict attention to a neighbourhood of the $(0, 1)$ resonance for perturbations of (1), but where θ denotes $pz - \sigma p' x$.

For all small perturbations of (1), $z = 0$ is a cross-section for y small, and we can consider the return map from $z = 0$ to $z = 1$. When α, β, ε and y are small, the motion in (x, y) is slow compared with that for z. Denote by ζ a bound on $(\dot{x}, \dot{y})$ for the region of interest. By the method of averaging, for all N up to the degree of differentiability of the vector field, the return map is within $O(\zeta^N)$ of the time-1 map of some parameter-dependent autonomous vector field on $\mathbb{T} \times I$. It will suffice for us to study a parameter regime with $\alpha = O(\varepsilon)$, $\beta = O(\sqrt{\varepsilon})$ and to take $y = O(\sqrt{\alpha})$, thus we can take $\zeta = \sqrt{\varepsilon}$, giving $O(\varepsilon^{N/2})$ accuracy. We call the result a 'flow approximation'.

The idea of the proof is that z can be taken as new time and a sequence of near-identity z-dependent coordinate changes in (x, y) constructed to reduce the dependence of $(\mathrm{d}x/\mathrm{d}z, \mathrm{d}y/\mathrm{d}z)$ on z to $O(\zeta^N)$. We leave out the details as it is a standard procedure (see [SV,GH,LM] and appendix B of [BGKM]).

Denoting the new variables by (X, Y), the result is approximation of the return map for perturbations of (1) for α, β, y small by the time-1 map of a family of autonomous vector fields

$$\begin{aligned} \dot{X} &= \beta + \frac{Y}{\gamma} + O(\varepsilon, Y^2) \\ \dot{Y} &= \alpha - Y^2 + O(\varepsilon, Y^3) \end{aligned} \tag{2}$$

where $\gamma > 0$ and the remainder terms are small in a norm of sufficiently high smoothness.

5. Minimum bifurcation structure for flow approximation

As a result of the previous two sections, for given (p, q) we can approximate the return map for perturbations of the system (1) near (p, q)-resonance to a high order in the perturbation ε by the time-1 map of a family of vector fields on $\mathbb{T} \times I$ of the form (2). This is the object of study for the present and next sections.

For ε small enough and α small but $\alpha > K\varepsilon$ for some K, the $\dot{Y}$ equation shows that there is an attractor–repellor pair located near $Y = \pm\sqrt{\alpha}$, respectively, and for $\alpha > K'\varepsilon$ for some $K' > K$, normal hyperbolicity in these two zones implies that the attractor and repellor are graphs of C^1 functions $X \mapsto Y$ (smoother for ε smaller). There is $K'' > 0$ such that for β more than $K''\varepsilon$ away from a curve near $\alpha = \gamma^2\beta^2$ the attractor and repellor are periodic orbits, both travelling to the left for β to the left of this zone in parameter space, to the right for β to the right, and in the intermediate region of β the upper one (attractor) travels to the right and the lower one (repellor) to the left.

For $\alpha < -K\varepsilon$ the $\dot{Y}$ equation shows that the non-wandering set Ω restricted to $|Y|$ of order $\sqrt{\alpha}$ is empty. For $|\beta| > K'''\sqrt{\varepsilon}$ for some K''' there is a transition as α decreases from $K\varepsilon$ to $-K\varepsilon$ from two periodic orbits to none via a curve of saddle-node of periodic orbits (snp) of the form α a smooth function of β. This is because (taking the case $\beta > 0$) the

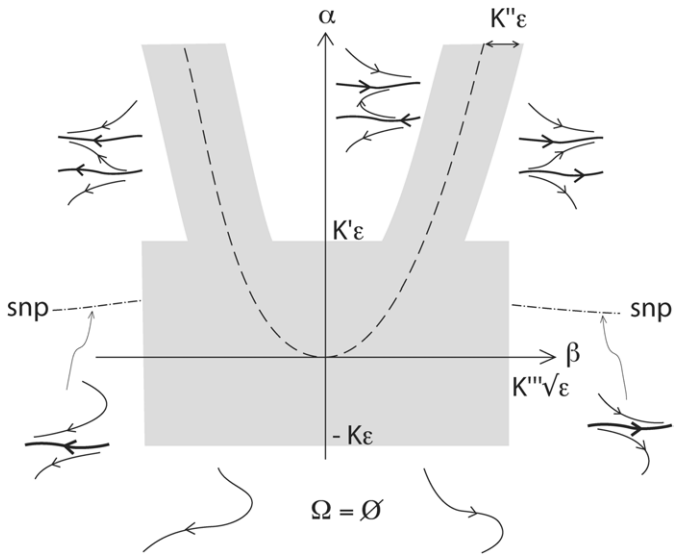

Figure 1. Outside the grey box and strips in parameter space, the dynamics of (2) has the indicated simple behaviour. snp = saddle-node of periodic orbits.

map from $X = 0$ to $X = 1$ is well approximated in C^2 by $Y' = Y + (\alpha - Y^2)/\beta$, which has a saddle-node curve of fixed points along $\alpha = 0$. The results so far are summarized in figure 1.

Next, consider the set of equilibria in the product of state space $\mathbb{T} \times I$ and parameter space $\mathbb{R}^2$. It is the graph of a differentiable map E from (X, Y) to (α, β), because in (2) the derivative of $(\dot{X}, \dot{Y})$ with respect to (α, β) is invertible. So the set of equilibria in the product space is a cylinder. The map E is approximately $\alpha = Y^2$, $\beta = -\frac{Y}{\gamma}$. Thus the set of parameter values (α, β) for which there is an equilibrium is the image of a smooth map from $\mathbb{T} \times I$ to $\mathbb{R}^2$ and lies near the curve $\alpha = \gamma^2\beta^2$. It is connected and the generic singularities of the map are fold curves connected at cusp points. The determinant of the derivative of the vector field at an equilibrium changes sign on crossing a fold curve. Negative determinant indicates a saddle, positive determinant an equilibrium of index +1 (node, spiral, improper node or centre).

The trace of the derivative of the vector field (2) is to leading order $-2Y$, which has non-zero derivative with respect to Y, so on the cylinder of equilibria there is a smooth homotopically non-trivial circle where the trace at the equilibrium is zero, separating equilibria with positive trace (for lower Y) from those with negative trace (for higher Y). For an equilibrium of index +1, positive trace indicates a repellor, negative trace an attractor and zero trace a Hopf bifurcation (generically). For a saddle, positive trace indicates that the repelling eigenvalue is stronger than the attracting one, and negative trace the other way round; the distinction is important in determining the outcome of homoclinic bifurcation. We call a saddle with trace zero a *neutral saddle*. This trace-zero circle on the cylinder of equilibria projects to a closed curve in parameter space connecting the boundaries of the image. Codimension-2 robustly, intersections of the image of the trace-zero curve with the image of a fold curve are Takens–Bogdanov points (*B points* in the terminology of [BGKM]) and they have quadratic tangency there.

Let us consider the simplest case for the map from the cylinder of equilibria to parameter space, namely that it has just two disjoint fold curves (saddle-node equilibria) and no cusp

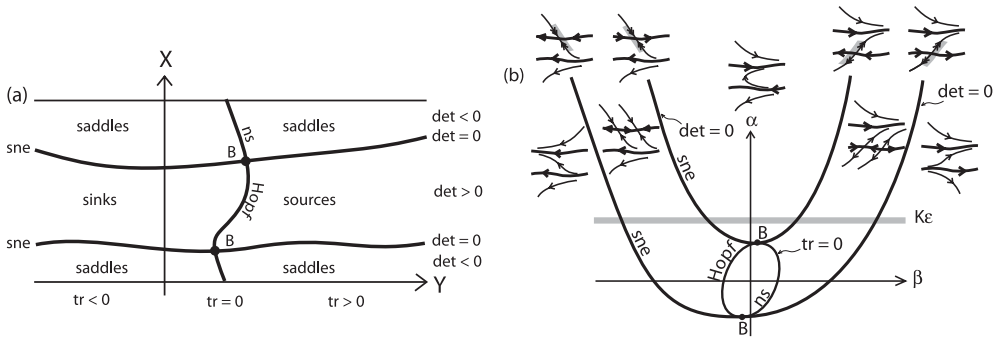

Figure 2. Simplest case for the set of equilibria: (*a*) as a graph over (Y, X) and (*b*) its image in parameter space (β, α), showing in each case the curve of $trace = 0$ equilibria with its two parts (Hopf and neutral saddle), and in the second case phase portraits in the normally hyperbolic domain. sne = saddle-node equilibrium, ns = neutral saddle.

points. See figure 2(*a*). Equivalently, in the world of codimension-2 robust phenomena, we suppose that for a given parameter value there are at most two equilibria. Then the set of parameters for which there is an equilibrium is a strip bounded by two smooth curves near the curve $\alpha = \gamma^2\beta^2$. For each point in the interior of the strip there are two equilibria: an index +1 point and a saddle.

Then the circle of trace zero equilibria projects to a closed curve with precisely one B point on each boundary of the strip. One half of the trace-zero curve separates the attracting equilibria from the repelling ones, via a Hopf bifurcation. The other half corresponds to neutral saddles (ns). The simplest case is that the two halves of trace-zero curve connecting the two B points do not intersect, as shown in figure 2(*b*). At the end of this section, however, we will consider the second simplest case, where they intersect once and transversely.

For large α (compared to ε) we already know that we have an attractor–repellor pair consisting of two C^1 graphs over X. Thus in the ends of the parameter strip for equilibria, the equilibria must lie on one or other of these two C^1-graphs. For $\beta < 0$ we have $trace < 0$ so the index 1 equilibrium is attracting, so it must lie on the upper invariant circle. The saddle must lie on the same circle, else we would have an invariant circle with no possible α-limit set for points other than the attracting equilibrium. Thus the upper circle contains an attracting equilibrium and a saddle, and the bottom one is a periodic orbit travelling to the left. Similarly, for $\beta > 0$ in the ends of the strip the lower circle contains a repelling equilibrium and a saddle and the upper circle is a periodic orbit travelling to the right. The results so far are summarized in figure 2.

Consider how these two situations can be connected by following the interior of the strip. Starting from the top left, the saddle and index 1 equilibrium must migrate from the upper invariant circle to the lower one. The only way this can be achieved codimension-1 robustly is by a pair of rotational homoclinic bifurcations (*rotational* means homotopically non-trivial), one producing a right-travelling periodic orbit above the saddle and index 1 point, the other producing a left travelling periodic orbit below them. Thus the strip is crossed by curves of homoclinic bifurcation of two types. Consideration of the sequence of events on the boundary of the strip (where the saddle and index 1 point collapse to a saddle-node equilibrium) shows that there are saddle-node loop bifurcation points (*Z points* in the terminology of [BGKM]) on which the curves of homoclinic bifurcation terminate with quadratic tangency to the fold curve, and their disposition with respect to the B points requires that the diagram have 'at least' the form of figure 3.

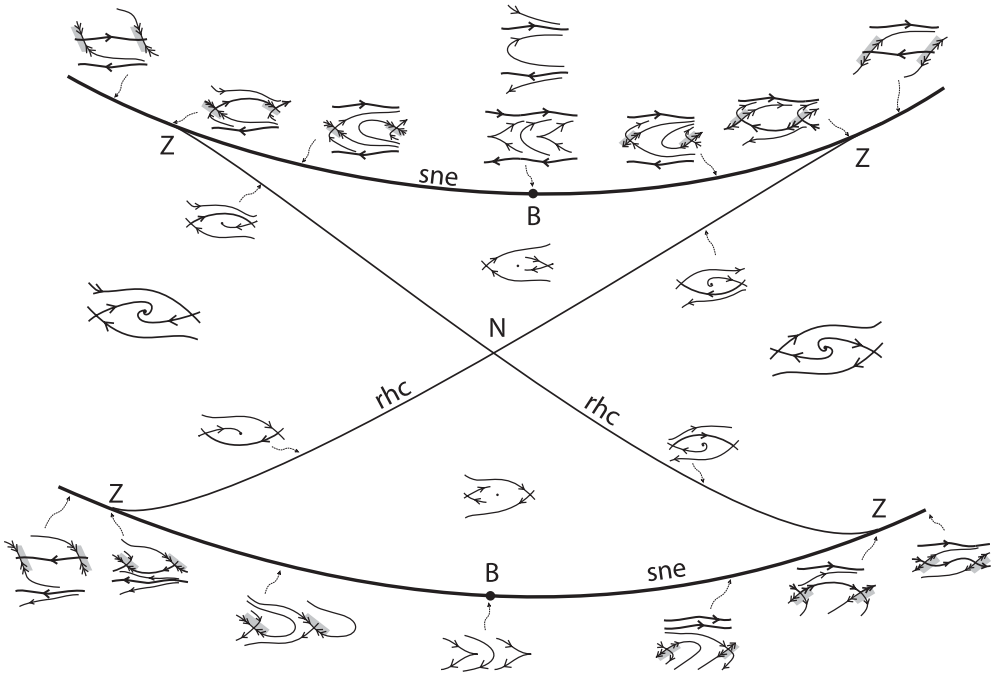

Figure 3. The simplest case for the curves of rotational homoclinic bifurcation (rhc).

In particular the curves of two types of rotational homoclinic bifurcation must cross. The codimension-2 robust way to do this is in a necklace point (*N point*) and we assume the simplest case of just one crossing. A necklace point produces two curves of contractible homoclinic bifurcation [BGKM]. Also the unfolding of each B point produces a curve of contractible homoclinic bifurcation (e.g. [GH]). These curves must connect to those from the necklace point, because there are no other places for them to end.

The rotational homoclinic bifurcation curves of figure 3 must cross the curve of neutral saddles of figure 2(*b*) somewhere. We suppose just once for simplicity. The stability of the periodic orbit produced in homoclinic bifurcation depends on the relative sizes of the eigenvalues of the saddle (attracting if their sum is negative, repelling if positive). Thus the periodic orbit changes stability on crossing the curve of neutral saddles; furthermore, the direction in parameter space in which homoclinic bifurcation produces a periodic orbit changes at such points. Following [BGKM] we call homoclinic bifurcation from a neutral saddle a *K point*. The codimension-2 robust unfolding of a K point contains a curve of saddle-node of periodic orbit, as shown in figure 4. These curves must extend to large positive and negative β, respectively, since the only way to eliminate the two periodic orbits for large positive α on passing to large negative α when β is large (so the flow is all in one direction) is saddle-node of periodic orbits. There could be cusp points in the snp curves, or isolas, but we suppose the simplest case in which these do not happen.

Hence we obtain minimal bifurcation diagram as in figure 5.

Note that there is a region in parameter space with three rotational periodic orbits (the wedge NKX, where X is an intersection of rhc and snp). It is not possible to make a robust bifurcation diagram with fewer. For example, the second simplest case is that the circle of $trace = 0$ equilibria maps to a curve in parameter space with one self-intersection. Figure 6

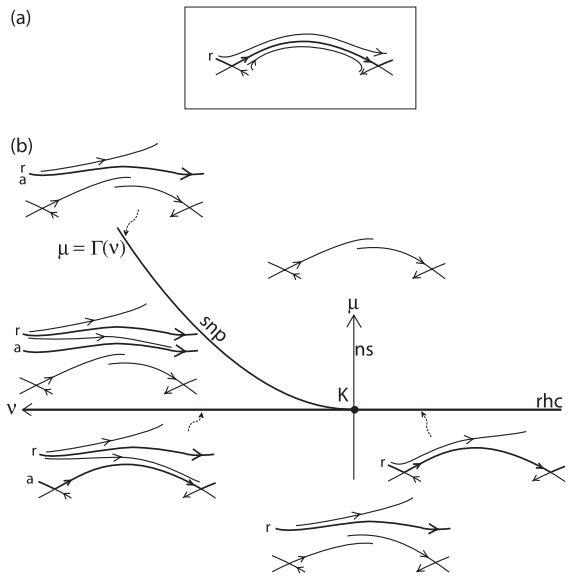

Figure 4. (*a*) Condition on phase portrait defining a K point (for the case when the homoclinic connection is weakly repelling). (*b*) Unfolding of the K point: as parameters we take the trace ν of the derivative at the saddle, and the amount μ by which the saddle connection is broken, measured in some transverse section. There is a curve of saddle-node of periodic orbits of the form $\mu = \Gamma(\nu)$, with $|\Gamma(\nu)| \leqslant e^{-C/\nu}$ for some $C > 0$ [DRS]. The case of a K point with weakly attracting homoclinic connection can be obtained by reflecting in ν, t and x.

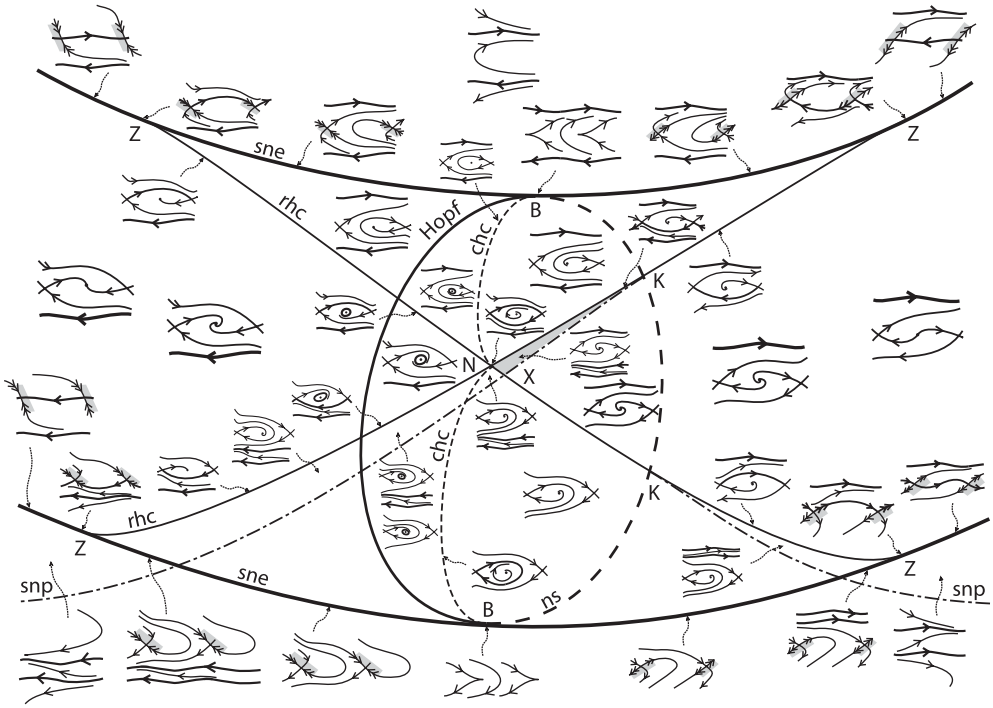

Figure 5. Simplest bifurcation diagram for the flow approximation for the return map near a low order resonance, with representative phase portraits.

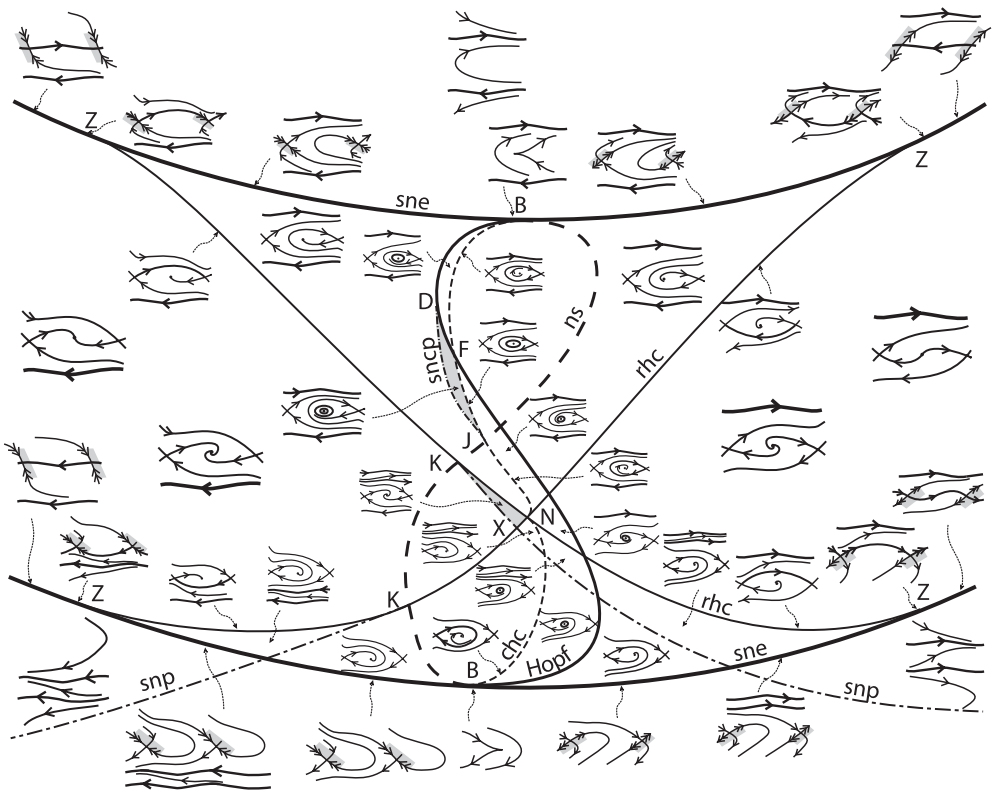

Figure 6. One second simplest bifurcation diagram, with a crossing of the curves of Hopf bifurcation and neutral saddle. It is drawn for the case when the N point falls inside the lower lobe of the trace = 0 curve. Of particular note is the necessary occurrence of a degenerate Hopf point (D) and associated triangle DFJ of existence of two contractible periodic orbits. There is again a wedge KNX with three rotational periodic orbits. Simplest diagrams of the same level of complication are obtained for the three other cases of position of the N point relative to the trace = 0 curve.

shows one way the resulting bifurcation diagram can look. Note that in addition to the features of the simplest case, this case is obliged to have a degenerate Hopf point (D) and a point of contractible neutral homoclinic connection (J), that are connected by a curve of saddle-node of contractible periodic orbits, and a region of two contractible periodic orbits (shaded triangle DFJ, where F is a crossing point of Hopf and contractible homoclinic bifurcation curves).

6. Shape of Chenciner bubble for flow approximation

Next we consider the Chenciner bubble for (2), namely the complement of the set of parameter values for which there is an attractor–repellor pair of C^1 invariant circles, or an invariant circle attracting from one side and repelling from the other, or empty non-wandering set locally.

The codimension-1 ways in which a C^1 invariant circle can be lost are saddle-node of periodic orbits, homoclinic bifurcation, 'rapid connection' (to be defined below) from a saddle to a node on the circle, and improper node on the circle. We have examined the first two already, thus it just remains to examine the latter two. They are not usually regarded as bifurcations,

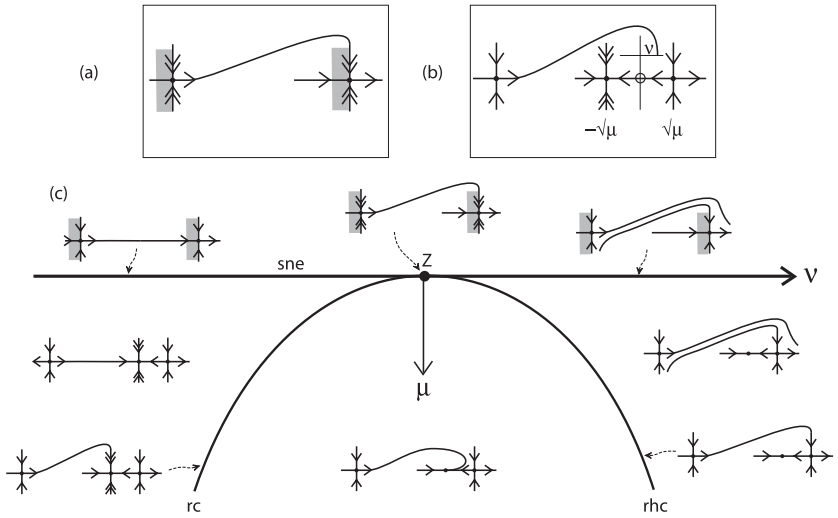

Figure 7. (*a*) The condition defining a Z point, (*b*) parameters (μ, ν) to unfold a Z point (μ unfolds the saddle node) and (*c*) the generic unfolding of a Z point, including a curve of rapid connection (rc).

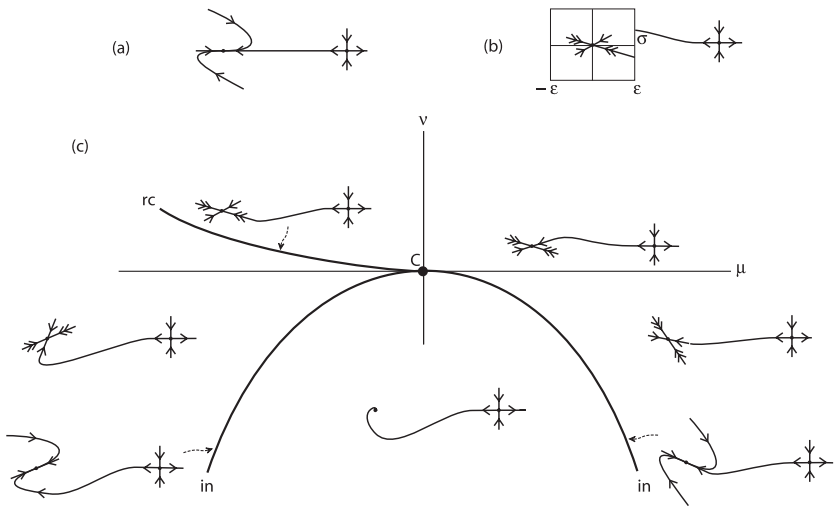

Figure 8. (*a*) Phase portrait defining an C point, (*b*) linearization box and definition of σ (see appendix) and (*c*) generic unfolding of an C point, including the curves of rapid connection (rc) and improper node (in).

because nothing changes at the C^0 level, but when C^1 considerations are important they play a significant role.

The condition for an improper node is $Tr^2 = 4Det$ for the derivative at an equilibrium. This includes the B points as a limiting case. Since Tr varies at a negative rate with respect to Y and hence positively with respect to β, we obtain a simple closed curve of improper node (in) in the strip, with quartic tangency to the fold curve at the B points.

We say there is a *rapid connection* (rc) from a saddle to a node if one branch of invariant manifold from the saddle comes into or leaves the node along its faster eigendirection. There

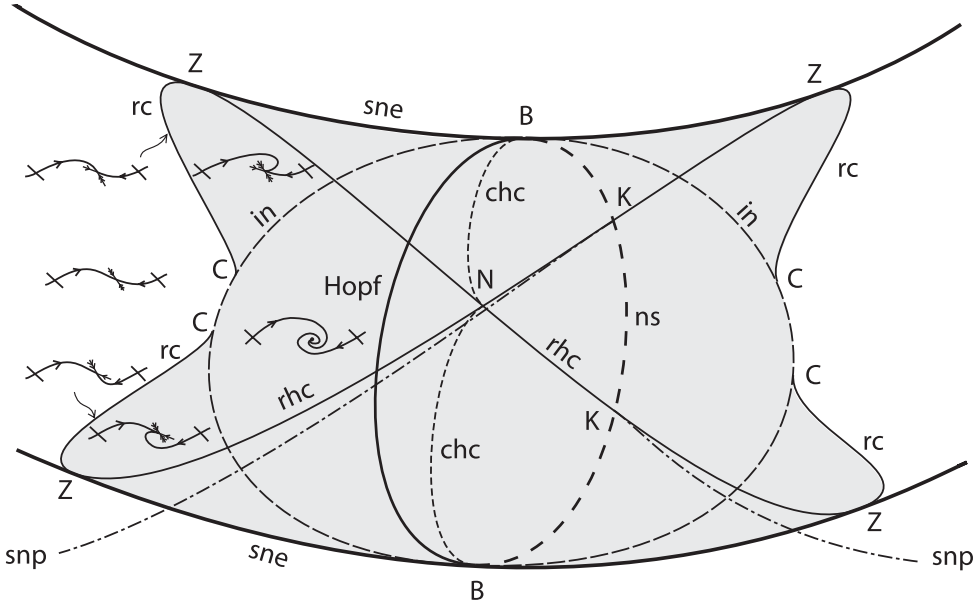

Figure 9. Simplest codimension-2 stable form for a Chenciner bubble (shaded grey), for the flow approximation of the return map near a low-order resonance. in = improper node, rc = rapid connection

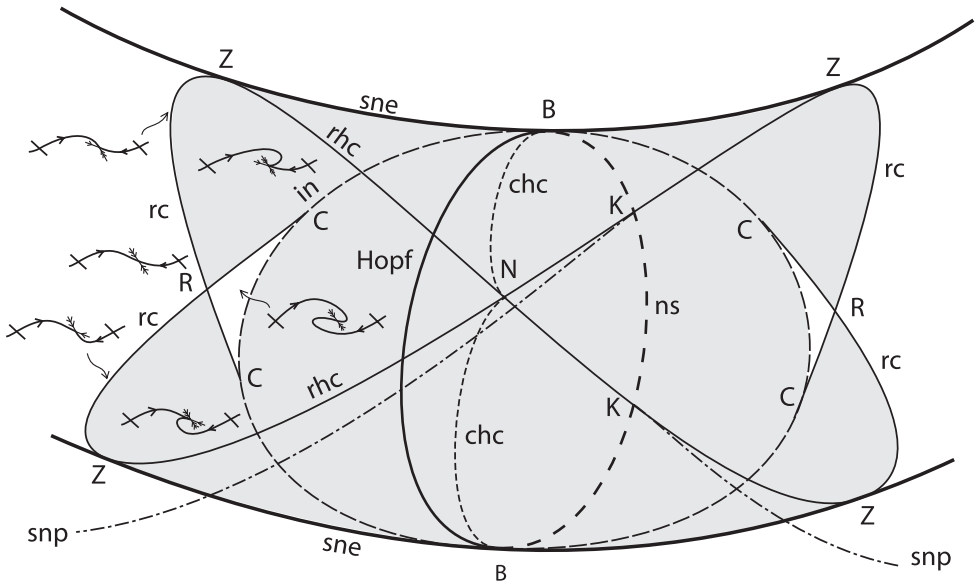

Figure 10. Second simplest form for a Chenciner bubble (shaded grey).

are curves of rapid connection coming out of each Z point, with quadratic tangency to the fold curve, continuing the curve of rotational homoclinic connection. The generic unfolding is shown in figure 7.

Where can the curves of rapid connection coming out of Z points end? They cannot connect different Z points, because the phase portraits there are not continuously deformable

into one another. The only place to end is at places we call *C points* where there is a C^2 connection from a saddle to an improper node. Recall that the generic trajectory into (or out of, if it is repelling) an improper node has curvature going to infinity at the end, but that the 'last' trajectory to go into the node on a given side does so with bounded curvature. The generic unfolding near a C point is indicated in figure 8; see appendix for the analysis. In particular, the curve of rapid connections comes in to a C point tangent to the curve of improper nodes. The behaviour in the wedge of tangency limits the ways this can fit in the rest of the diagram.

Thus the simplest shape for a Chenciner bubble is that of figure 9.

The second simplest shape involves one or both pairs of curves of rapid connection crossing in an *R point* where there are rapid connections from a saddle into both sides of a node. Such a case is shown in figure 10. Note that there are pockets of parameter values with an attractor–repellor pair of C^1 circles surrounded by the Chenciner bubble, though the circles are not graphs over X. The diagram need not have R points on both sides; perhaps the cases with an R point on just one side should be regarded as simpler. Note that introducing self-intersections of the curve of trace-zero equilibria does not affect the shape of the Chenciner bubble.

7. Comparison with Chenciner's case

The family of vector fields that Chenciner [Ch] obtained as a leading order flow approximation near resonance in the unfolding of a Neimark–Sacker bifurcation is

$$\begin{aligned} \dot\theta &= y \\ \dot y &= \bar\alpha + \bar\beta y + \gamma y^2 + \delta\cos 2\pi\theta, \end{aligned} \tag{3}$$

where we have put bars over some parameters to distinguish them from ours (but γ will correspond exactly). In the variables $Y = -\gamma y - \frac{\bar\beta}{2}$, $X = -\theta$, and parameters $\alpha = \frac{\bar\beta^2}{4} - \gamma\bar\alpha$, $\beta = \frac{\bar\beta}{2\gamma}$ and $\varepsilon = -\gamma\delta$, (3) transforms to a system of our form (2) with a specific perturbation:

$$\begin{aligned} \dot X &= \beta + \frac{Y}{\gamma} \\ \dot Y &= \alpha - Y^2 + \varepsilon\cos 2\pi X. \end{aligned} \tag{4}$$

We will treat it in Chenciner's variables and follow his convention that $\gamma < 0$ (opposite to what we have used so far), and $\delta > 0$ (note that δ can be scaled to 1).

Its bifurcation diagram [CGL] (reproduced in [Ch]) is like our simplest one (figure 5) but it has the exceptional features that the circle of trace-zero equilibria projects to a single line crossing the strip transversely (in fact, the line $\bar\beta = 0$), the N point lies on this line, and on this line the dynamics on the universal cover is Hamiltonian. Thus our curves of Hopf bifurcation, neutral saddle and contractible homoclinic bifurcation all collapse onto this line, the K points collapse onto the N point, which changes to a version of infinite codimension, and the B points change to infinite codimension versions.

Aspects of how the bifurcation diagram of [CGL] should be modified when generic higher order terms are included were proposed by Chenciner [Ch], and they fit with what we have obtained here. In particular, he found a curve of Hopf bifurcation and two curves of contractible homoclinic bifurcation, and commented that it is possible to produce a degenerate Hopf point.

For small γ, the boundary of the Chenciner bubble for Chenciner's family (3) is like our simplest one (figure 9), as we now prove.

First note the symmetry $(\bar\beta, y, t) \mapsto (-\bar\beta, -y, -t)$, so it suffices to study one side of the diagram, say $\bar\beta < 0$. If in addition, $\bar\beta^2 > 8\pi\delta$ then the linearized dynamics in $y \geqslant 0$ has a forward invariant cone (cf [Le]), $\{(\theta', y') : \theta' > 0,\ y' > \frac{\bar\beta}{2}\theta'\}$ (where (θ', y') denotes a tangent vector), as can be checked by showing $\dot\theta' > 0$ on $\{\theta' = 0,\ y' > 0\}$, and $\dot y' - \frac{\bar\beta}{2}\dot\theta' > 0$ on $\{y' = \frac{\bar\beta}{2}\theta', \theta' > 0\}$. This precludes existence of a connection from the saddle going into the node along the rapid direction from $y > 0$, since the trajectory would have to be entirely in $y > 0$ and the rapid eigenvector is outside the cone. So for all $\gamma < 0$, the curve of rapid connection from the upper left Z point is constrained to be in the region $\bar\beta > -\sqrt{8\pi\delta}$. But the curve of improper nodes is $\frac{\bar\beta^4}{64\pi^2} + \bar\alpha^2 = \delta^2$, so the curve of rapid connection from the upper left Z point is constrained to the region $\bar\alpha > 0$, $\bar\beta > -\sqrt{8\pi\delta}$.

Next, note that for $\gamma = 0$ there is the additional symmetry $(\bar\alpha, y, \theta) \mapsto (-\bar\alpha, -y, \frac{1}{2} - \theta)$, so for γ small the curve of rapid connection from the lower left Z point is close to being the reflection of that from the upper left Z point. Thus for γ small the two curves of rapid connection do not intersect. In particular, for γ small we confirm Chenciner's diagram, with the exception that we establish the orders and directions of contact of the curves of rapid connection which he and [CGL] did not address.

For large γ there is the possibility of R points; we have not decided this either way but give a short discussion of how the question might be tackled. The $\dot y = 0$ nullcline is a slow manifold away from its possible intersections with $y = -\frac{\bar\beta}{2\gamma}$, since the derivative $\frac{\partial\dot y}{\partial y} = \bar\beta + 2\gamma y$ is large compared with $\dot\theta = y$. For $\bar\alpha - \frac{\bar\beta^2}{4\gamma}$ significantly less than δ the $\dot y = 0$ nullcline has an upper connection from the saddle to the sink but no lower connection. For $\bar\alpha - \frac{\bar\beta^2}{4\gamma}$ significantly greater than δ the $\dot y = 0$ nullcline consists of two C^1 graphs over θ, the upper one connecting the saddle and sink both ways (the lower one having unidirectional flow to the left). So the only region of parameter space where rotational homoclinic bifurcation, necklace point, saddle-node of rotational periodic orbits, Z points and rapid connections can occur is a neighbourhood of the curve $\bar\alpha - \frac{\bar\beta^2}{4\gamma} = \delta$. This passes through the upper B point and crosses the lower saddle-node of equilibria curve ($\bar\alpha = -\delta$) at $\bar\beta = \pm\sqrt{8|\gamma|\delta}$. Thus the lower Z points are at much larger $\bar\beta$ than the upper ones and the curves of rapid connection from the lower Z points are obliged to continue into $\bar\alpha > 0$. So it is possible that the two curves of rapid connection might cross for large enough γ.

8. Effects of deviation from flow approximation

Finally, we address the effects of deviations of the return map to $z = 0$ from the time-1 map of the flow approximation. Since the deviation can be pushed to arbitrarily high order in $(\varepsilon, \alpha, \beta)$ (subject to sufficient smoothness), the effects are small. But generically, we have to expect that the curves of rotational homoclinic bifurcation are fattened into strips, the Z points are fattened into intervals in the saddle-node curves, the N point is fattened into a rectangle, the curves of contractible homoclinic bifurcation are fattened into strips (tapering to wedges at the B points), the curves of rapid connection are fattened into strips where some orbits on one branch of invariant manifold of the saddle come into the node along its rapid direction, the C points are fattened into intervals in the curve of improper nodes and finally, the curves of saddle-node of periodic orbit are fattened into strings of Chenciner bubbles for resonances of low enough order compared with the error in the flow approximation, interpolated by more complicated zones and possibly some good Diophantine points where the saddle-node of tori proceeds as if for the flow approximation (Chenciner's good paths). The simplest result is shown in figure 11.

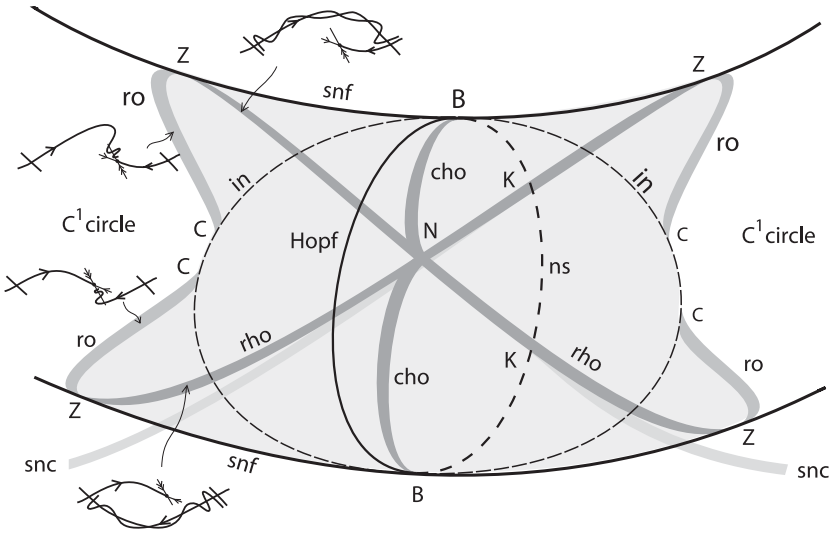

Figure 11. The effect on the bifurcation diagram and Chenciner bubble of typical deviation of the return map from the time-1 map of the flow approximation. snf = saddle-node fixed point, Hopf = Neimark–Sacker fixed point, rho/cho = rotational/contractible homoclinic orbit, ro = existence of an orbit between a saddle and the rapid direction of a node and snc = zone of transition between two invariant circles and none.

9. Conclusion

We have shown that the picture obtained by Chenciner near resonance in the unfolding of a degenerate Neimark–Sacker bifurcation generalizes to a more global context, but that some non-generic features of his flow approximation are lifted in general and the bifurcation diagrams are more complicated. We have given the simplest robust bifurcation diagram and Chenciner bubble.

One application is to the boundaries of partial mode-locking regions for three coupled oscillators. In place of a curve of saddle-node periodic orbits of given homotopy type on the 2-torus for a flow approximation, one should expect to see strings of Chenciner bubbles with structure at least that of our simplest one here.

Acknowledgments

Alain Chenciner's lectures on the degenerate Neimark–Sacker bifurcation at the Les Houches school on Deterministic Chaos in 1981 were a formative experience for both the authors. They are grateful to Seunghwan Kim for producing useful numerical confirmation of their initial results, just after a visit of him to them in Cambridge in 1997 (and to EPSRC and the British Council for supporting his visit). The authors finished the project during a sabbatical leave at IHES (France) in 2006, for whose hospitality they are most grateful.

Appendix. Unfolding of a C point

In this appendix we derive the generic unfolding of a C point, that is a phase portrait with an attracting improper node and a branch of unstable manifold of a saddle coming into the node on the boundary of the set of trajectories coming in from one side (as in figure 8(*a*)).

Choose coordinates and time scale so that the derivative at the improper node at the C point is $\begin{bmatrix} -1 & 1 \\ 0 & -1 \end{bmatrix}$. Unfolding this by adding general perturbation $\begin{bmatrix} a & b \\ c & d \end{bmatrix}$ yields a codimension-1 manifold

$$\Delta = \frac{1}{4}(a-d)^2 + c(1+b) = 0$$

of improper nodes. The fast eigenvector (take the unique one when the node is improper) is proportional to $\begin{bmatrix} 1+b \\ \frac{d-a}{2} - \sqrt{\Delta} \end{bmatrix}$. There exists a smooth coordinate change depending smoothly on parameters (C^1 suffices for us) to linearize the vector field in a neighbourhood N of a node [IY2], without loss of generality a rectangle $[-\epsilon, \epsilon] \times [-\eta, \eta]$ in the linearizing coordinates (x, y). Let σ be the height y in the linearizing coordinates at which the branch of unstable manifold of the saddle enters N (without loss of generality on $x = \epsilon$; see figure 8(b)). It is a C^1 function of parameters.

Take a two-parameter family of perturbations of the C point with parameters (μ, ν) and suppose that the derivative of the mapping $(\mu, \nu) \mapsto (\frac{a-d}{2}, c)$ has full rank so without loss of generality

$$\mu = \frac{a-d}{2}, \qquad \nu = c.$$

The condition for a rapid connection from the saddle to the node is

$$\epsilon \frac{(-\mu - \sqrt{\Delta})}{1+b} = \sigma. \tag{5}$$

The height $\sigma = A\mu + B\nu + o(\mu, \nu)$ for some $A, B \in \mathbb{R}$, and $\Delta = \mu^2 + (1+b)\nu$, so (5) can be rewritten as

$$\sqrt{\mu^2 + (1+b)\nu} \sim -A'\mu - B'\nu, \tag{6}$$

where $A' = \frac{A}{\epsilon} + 1$ and $B' = \frac{B}{\epsilon}$. It follows that there is a rapid connection if and only if

$$\nu \sim \frac{1}{1+b}[(A'\mu + B'\nu)^2 - \mu^2] \qquad \text{and} \qquad A'\mu + B'\nu \leqslant 0. \tag{7}$$

Assume that $A' \neq 0$, without loss of generality $A' > 0$ (by reflecting in y and μ). Then the implicit function theorem gives a curve of rapid connection

$$\nu \sim (A'^2 - 1)\mu^2, \qquad \mu < 0. \tag{8}$$

The bifurcation diagram is completed by adding the phase portraits as in figure 8(c).

References

[AY] Afraimovich V S and Young T 2000 Mather invariants and smooth conjugacy on $\mathbb{S}^2$ *J. Dyn. Control Sys.* **6** 341–52

[AF] Asimov D and Franks J 1983 Unremovable closed orbits *Geometric dynamics (Lecture Notes in Maths* vol 1007*)* ed J Palis (Berlin: Springer) pp 22–9

[BGKM] Baesens C, Guckenheimer J, Kim S and MacKay R S 1991 Three coupled oscillators: mode-locking, global bifurcations and toroidal chaos *Physica* D **49** 387–475

[BGKM2] Baesens C, Guckenheimer J, Kim S and MacKay R S 1991 Simple resonance regions of torus diffeomorphisms *Patterns and Dynamics in Reactive Media Proc. IMA (Minneapolis, 1989) (IMA Vol. in Maths and its Applications)* vol 37, ed R Aris *et al* (Berlin: Springer) pp 1–9

[BNRSW] Broer H W, Naudot V, Roussarie R, Saleh K and Wagener F O O 2007 Organising centres in the semi-global analysis of dynamical systems *Int. J. Appl. Math. Stat.* in press

[Ch] Chenciner A 1988 Bifurcations de points fixes elliptiques: III. Orbites périodiques de ≪petites≫ périodes et élimination résonnante des couples de courbes invariantes *Publ. Math. IHES* **66** 5–91

[CGL] Chenciner A, Gasull A and Llibre J 1987 Une description complète du portrait de phase d'un modèle d'élimination résonante *C. R. Acad. Sci. Paris Sér I* **305** 623–6

[Co] Conley C 1988 The gradient structure of a flow: I *Ergod. Theory Dynam. Syst.* **8** 11–26

[DRS] Dumortier F, Roussarie R and Sotomayor J 1987 Generic three parameter families of vector fields on the plane, unfolding a singularity with nilpotent linear part: the cusp case of codimension 3 *Ergod. Theory Dynam. Syst.* **7** 375–413

[Fr] Fried D 1982 Flow equivalence, hyperbolic systems and a new zeta function for flows *Commun. Math. Helv.* **57** 237–59

[GH] Guckenheimer J and Holmes P J 1990 *Nonlinear Oscillations, Dynamical Systems and Bifurcation of Vector Fields* 2nd edn (Berlin: Springer)

[Ha] Handel M 1985 Global shadowing of pseudo-Anosov homeomorphisms *Ergod. Theory Dynam. Syst.* **5** 373–7

[IY] Il'yashenko Yu S and Yakovenko S Yu 1993 Nonlinear Stokes phenomena in smooth classification problems *Nonlinear Stokes Phenomenon* ed Yu S Ilyashenko *Adv. Sov. Math.* **14** 235–87

[IY2] Il'yashenko Yu S and Yakovenko S Yu 1991 Finitely-smooth normal forms of local families of diffeomorphisms and vector fields *Russ. Math. Surv.* **46** 1–43

[Le] Levi M 1988 Nonchaotic behavior in the Josephson junction *Phys. Rev.* A **37** 927–31

[LM] Lochak P and Meunier C 1988 *Multiphase Averaging for Classical Systems* (Berlin: Springer)

[SV] Sanders J A and Verhulst F 1985 *Averaging Methods in Nonlinear Dynamical Systems* (Berlin: Springer)

[TW] Takens F and Wagener F O O 2000 Resonances in skew and reducible quasi-periodic Hopf bifurcation *Nonlinearity* **13** 377–96

[Yo] Yoccoz J-C 1987 Bifurcation de points fixes élliptiques (d'après A Chenciner) *Séminaire Bourbaki* no 668 in *Astérisque* **145–146** 313–34